ELSEVIER SCIENCE IRELAND

Chemistry and Physics of Lipids
69 (1994) 75–85

Chemistry and Physics of LIPIDS

Fluorescence study of a derivatized diacylglycerol incorporated in model membranes

M.J.E. Prieto[a], M. Castanho[a], A. Coutinho[a], A. Ortiz[b], F.J. Aranda[b], J.C. Gómez-Fernández*[b]

[a]*Centro de Química Física Molecular, IST, 1096 Lisboa Codex, Portugal*
[b]*Departamento de Bioquímica y Biología Molecular A, Facultad de Veterinaria, Universidad de Murcia, Aptdo. 4021, E-30080 Murcia, Spain*

(Received 29 March 1993; revision received 23 June 1993; accepted 5 July 1993)

Abstract

A fluorescence study of a diacylglycerol derivatized with the *n*-(7-nitrobenz-2-oxa-1,3-diazol-4-yl) chromophore (NBD) was carried out. Fluorescence self-quenching was observed for this probe in lecithin model membranes due to collisional interaction rather than to an aggregational behaviour of the probe. The efficient energy migration ($R_0 = 28$ Å) of the NBD fluorophore was studied via the fluorescence depolarization upon increase of probe concentration in membranes, and the results are compared with a model where a random distribution of the probes is assumed. A surface location of the chromophore was concluded for the NBD derivative of diacylglycerol, both from the fluorescence parameters and from the study of its fluorescence quenching by spin label probes. Very high lateral diffusion coefficients were obtained for these probes, both from the self-quenching ($D = 2\text{–}6 \times 10^{-6}$ cm^2 s^{-1}) and from the spin probe quenching ($D = 3.5 \times 10^{-6}$ cm^2 s^{-1}) studies. A concomitant fluorescence study of the related probe NBD-phosphatidylcholine revealed that its photophysical behaviour is similar to the derivatized diacylglycerol.

Key words: NBD-Dioleoylglycerol; Phospholipid vesicles; Fluorescence

1. Introduction

Diacylglycerols (DG) are known to have a relevant role in several biochemical processes, namely activation of protein kinase C [1], alteration of membrane structure [2] and eliciting a great variety of biological activities [3]. Given the physiological importance of DG, we have obtained a fluorescent derivative that could be used to study more of its role as a bioactive lipid. In the present work we used a DG derivatized with the fluorescent chromophore NBD (Fig. 1). For this new probe we will present (i) its photophysical characterization in homogeneous and heterogeneous media, (ii) a study of its distribution func-

* Corresponding author.

Abbreviations: DPPC, dipalmitoylphosphatidylcholine; EYL, egg yolk lecithin; NBD, 7-nitrobenzo-2-oxa-1,3-diazol-4-yl; NBD-DG, 1-oleoyl-2-hexanoyl-NBD-glycerol; NBD-PC, 1-oleoyl-2-hexanoyl-NBD-phosphatidylcholine; *n*-NS, *n*-(*N*-oxy-4,4-dimethyloxazolidin-2-yl)stearic acid; PS, bovine brain phosphatidylserine

SSDI 0009-3084(93)02250-U

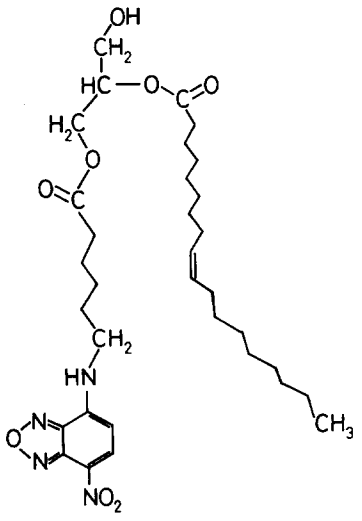

Fig. 1. Chemical structure of the diacylglycerol fluorescent derivative 1-oleoyl-2-hexanoyl-NBD-glycerol.

tion (information of distances) when incorporated in model membranes, via energy transfer (migration) and (iii) information on its dynamics (lateral diffusion) in model membranes via fluorescence self-quenching and from quenching by lipophylic nitroxide probes.

In order to evaluate specific effects that could be due to the presence of the chromophore (NBD) and not ascribed to the DG structure, the concomitant study of a derivatized standard phosphatidylcholine (NBD-PC) was also carried out.

2. Materials and methods

1-Oleoyl-2-hexanoyl-NBD-glycerol (NBD-DG) (Fig. 1) was synthesized for us by Lipid Products, Surrey, UK. 1-Oleoyl-2-hexanoyl-NBD-phosphatidylcholine (NBD-PC), egg yolk lecithin, bovine brain phosphatidylserine and dipalmitoyl-phosphatidylcholine were obtained from Avanti Polar Lipids Inc., Birmingham, AL, USA. 5-Doxylstearate and 16-doxylstearate were obtained from Sigma, Poole, Dorset, UK. Spectroscopic-grade organic solvents were purchased from Merck, Darmstadt, Germany. Twice-distilled and deionized water was used.

Phospholipid vesicles were made as follows: chloroform solutions containing the phospholipid and the appropriate amount of NBD-DG or NBD-PC were mixed, the organic solvent removed under a stream of dry N_2 and last traces removed by a further evaporation under vacuum. Multilamellar vesicles (MLV) were formed by addition of 0.1 mM EDTA, 100 mM NaCl, 5 mM Hepes, pH 7.4 buffer and mixing using a bench vibrator.

Samples for fluorescence quenching of the NBD-derivative by spin label nitroxides were performed as follows: MLV containing phospholipid and the NBD-derivative prepared as described above were extruded through two stacked polycarbonate filters (Nuclepore, 0.1 μM pore size) using an extruder (Lipex Biomembrane Inc., Vancouver, Canada) to form large unilamellar vesicles (LUV). To these LUV the nitroxide probes were added from an ethanolic stock solution. No alteration of the bilayer structures is reported, even for the highest amount of ethanol added, 3% [4]. Lipid vesicle samples were analyzed for organic phosphorous by the method of Bartlett [5]. Probe concentrations were calculated using a molar extinction coefficient in ethanol $\epsilon = 2.24 \times 10^4$ M^{-1} cm^{-1} ($\lambda = 465$ nm) [6].

Absorption spectra were recorded on a Perkin-Elmer Lambda 15 spectrophotometer, using 1 cm path cuvettes.

Steady-state excitation and emission spectra were carried out using 5 mm × 5 mm cuvettes in a Spex F112 A Fluorolog spectrofluorometer with a double emission monochromator and a thermostating unit. Excitation and emission bandwidths were 1.8 and 2.25 nm, respectively. Correction of excitation and emission spectra were performed using a rhodamine B quantum counter solution and a standard lamp, respectively [7].

Fluorescence self-quenching, anisotropy and the nitroxide (*n*-NS) quenching measurements were carried out on a Spex F112 A Fluorolog or on a Shimadzu RF-540 spectroflurometer, using excitation and emission wavelengths of 462 and 543 nm, respectively.

All the fluorescence measurements were carried out in a right-angle geometry, and the eventual artefacts arising in a steady-state experimental approach were taken into account.

Fluorescence quantum yields were determined vs. diphenylanthracene in cyclohexane ($\phi_f = 0.90 \pm 0.02$ [7]). Fluorescence measurements in lipid solutions were obtained in a magic angle arrangement, to avoid polarization bias of intensity. Fluorescence anisotropies were determined from Eq. 1, where I_{vv} and I_{vh} are fluorescence intensities, the two subscripts indicating the orientation of the excitation and emission polarizers, respectively, and $G = I_{hv}/I_{hh}$ is the instrumental factor. Glan-Thompson polarizers were used, the excitation and emission wavelengths were 462 and 543 nm, respectively, and 'blank' intensities were taken into account.

$$r = (I_{vv} - G\ I_{vh})/(I_{vv} + 2G\ I_{vh}) \quad (1)$$

Fluorescence decays were measured using the Single Photon Timing technique. The excitation source was a nitrogen-filled flash-lamp (Edinburgh Instruments, 119F), operated at 80 KHz. Excitation ($\lambda = 337$ nm) and emission ($\lambda = 543$ nm) wavelengths were selected with monochromators (Jobin Yvon, H20), with band-passes of 8.0 and 10.0 nm, respectively. Collection of pulse and sample profiles, detected with a cooled (−30°C) Philips XP2254 B photomultiplier, was alternated with maximum cycle times of 15 min. The sample temperature was controlled up to ±0.1°C. Decays were observed for three decades of intensity, with 0.122 ns/channel resolution, and 10 K counts were accumulated in the peak channel. Data analysis was performed with the δ-function convolution method [8], using Rose Bengal ($\tau = 500$ ps) as a reference [7], in order to avoid the 'color' effect of the photomultiplier. The best fit parameters (lifetimes, τ, and pre-exponentials, a) were obtained from a non-linear least-squares iterative program, minimizing χ^2. The adequacy of the fit to the decay data was judged from the χ^2 value and inspection of the weighted residuals plots.

Fluorescence decays were in general complex and described by two exponentials, the mean lifetime, τ, being obtained from Eq. 2:

$$\bar{\tau} = \Sigma a_i\ \tau_i^2/\Sigma a_i\ \tau_i \quad (2)$$

3. Theory

In the energy transfer studies, the critical radius of transfer, R_o, was evaluated from Försters's formula [9], rewritten as:

$$R_o = 0.02108\ [k^2\ \phi_D\ n^{-4} \int_o^\infty I(\lambda)\ \epsilon(\lambda)\ \lambda^4\ d\lambda]^{1/6} \quad (3)$$

with R_o in nm, where k^2 is the orientational factor, ϕ_D is the donor quantum yield in the absence of the acceptor, n is the refractive index of the medium, $I(\lambda)$ is the normalized fluorescence spectrum, $\epsilon(\lambda)$ is the molar absorption coefficient in $M^{-1}\ cm^{-1}$ and λ is in nm. In the above expression the orientational factor corresponding to a dynamic isotropic regime of transfer, $k^2 = 2/3$, was assumed; and $n = 1.36$ (ethanol), taken from the solvatochromic response of the chromophore (see Results), was considered.

For the purpose of surface concentration determination in the energy transfer experiments, a value of 77 $Å^2$ was considered for the area of phospholipid headgroup of EYL [10].

The extent of collisional quenching in a lipid bilayer depends upon the lipid/water partition coefficient and upon the rate of diffusion of the colliding species in the lipid bilayer [11]. Therefore the collisonal quenching of fluorescence can be used for calculating the diffusion coefficient for NBD-DG in lipid vesicles. In a membrane, where quenching occurs only in the lipid phase and quencher partition in the water phase may be significant, the following applies:

$$1/k_{app} = \alpha_m\ (1/k_m - 1/k_m\ P) + 1/k_m\ P \quad (4)$$

where k_{app} is the apparent (measured) bimolecular quenching constant in $M^{-1}\ s^{-1}$, α_m is the fractional volume of the membrane phase, and P is the partition coefficient, in units of (moles of quencher per volume of phospholipid)/(moles of quencher per volume of water). A plot of $1/k_{app}$ as a function of α_m gives a straight line with $1/k_m\ P$ as intercept and $(1/k_m - 1/k_m\ P)$ as slope. In order to estimate the lateral diffusion coefficients of NBD probes in the membrane we have used the Smoluchowski equation, taking into account transient effects [12]:

$$k_m = 4\,\pi\,N_A R_{pq}\,\gamma\,(D_p + D_q)\,(1 + R_{pq}\,\gamma/\sqrt{((D_p + D_q)\,\tau_0)} \quad (5)$$

where γ is the quenching efficiency parameter of the reaction, R_{pq} is the sum of the molecular radii of probe plus quencher, N_A is Avogadro's number per millimole, D_p and D_q are the diffusion coefficients of the probe and quencher, respectively, in the membrane, in units of $cm^2\ s^{-1}$ and τ_o is the fluorescence lifetime of the probe in the absence of quencher.

From the van der Waals radii we estimate a molecular radius of 4.3 Å for NBD-DG and 4.6 Å for 5-NS [13]. We have assumed $\gamma = 1$, as there is evidence that nitroxide quenching is an efficient process [14]. Anyway, a precise knowledge of γ is not essential regarding the dynamic information to be derived, i.e. the diffusion coefficients to be obtained are a lower bound. The lifetime for this probe is $\tau_o = 6.4$ ns; and $D_q = 2.5 \times 10^{-7}\ cm^2\ s^{-1}$ for a similar fluid membrane [15] was assumed.

Collisional self-quenching is described by the following kinetic scheme:

$$F + h\,\nu \longrightarrow F^* \quad (I_a) \quad (6)$$

$$F^* \xrightarrow{k_f} F + h\,\nu \quad (k_f[F^*] = I_f) \quad (7)$$

$$F^* + F \xrightarrow{k_m} F + F \quad (k_m[F^*][F]) \quad (8)$$

$$F^* \xrightarrow{k_d} F \quad (k_d[F^*]) \quad (9)$$

(F is the fluorophore, I_a is the intensity of absorbed light, k_f and k_d are the radiative and non-radiative rate constants and k_m the bimolecular self-quenching rate constant). If the concentration of F, $[F]$, is low enough to hold a linear Lambert-Beer relationship, then

$$I_a = I_o\,\epsilon\,[F]\,l \quad (10)$$

(ϵ, molar absorptivity; l, light path; I_o, intensity of incident light), and in steady-state conditions the fluorescence intensity is given by

$$I_f = k_f\,[F^*] = I_o\,\epsilon\,k_f\,l\,[F]/(k_f + k_d + k_m\,[F]) \quad (11)$$

or

$$1/I_f = k_m/(I_o\,\epsilon\,l\,k_f) + (k_f + k_d)/(I_o\,\epsilon\,l\,k_f)\ 1/[F] \quad (12)$$

Once the probe lifetime at infinite dilution is known, from the slope and intercept of Eq. [12] k_m can be determined.

4. Results and discussion

4.1. Photophysical characterization

In Fig. 2 the corrected excitation and emission spectra of NBD-DG incorporated in EYL vesicles are shown. The spectra show no significant vibrational resolution, and a strong overlap between them is observed.

Table 1 summarizes the maximum excitation and emission wavelengths, steady state anisotropy, r (dilute solutions) and mean fluorescence lifetimes ($\bar{\tau}$) of NBD-DG in homogeneous solvents and incorporated in several model systems of membranes. The probe displays a solvatochromatic effect, the energies of the excited (absorption) and relaxed (fluorescence) states being very dependent on the medium polarity. A concomitant dependence of the quantum yield was observed (results not shown), a very low value being obtained for water ($\phi < 10^{-3}$).

The lifetimes are complex, being in general described by two exponentials even in the case of homogeneous solvents. This effect is more evident when the probes are incorporated in lipid bilayers, and for EYL at 25°C, for example, the components are $\tau_1 = 3.55$ ns ($a_1 = 0.23$) and $\tau^2 = 6.84$ ns ($a_2 = 0.77$). The mean lifetimes are also solvent-dependent, the shortest one being obtained in water, and, as expected, the anisotropy values in homogeneous solvents are quite low. For the quantum yield, ϕ, of NBD-PC incorporated into EYL vesicles a value $\phi = 0.48$ was obtained.

While the NBD probes have been intensively used in biochemistry [16], its complex photophysics has not been reported in detail. This probe shows a very strong solvent response of its fluorescence parameters. As shown in Table 1, a red-shift of the emission upon increasing the solvent polarity is observed, this being compatible with a large

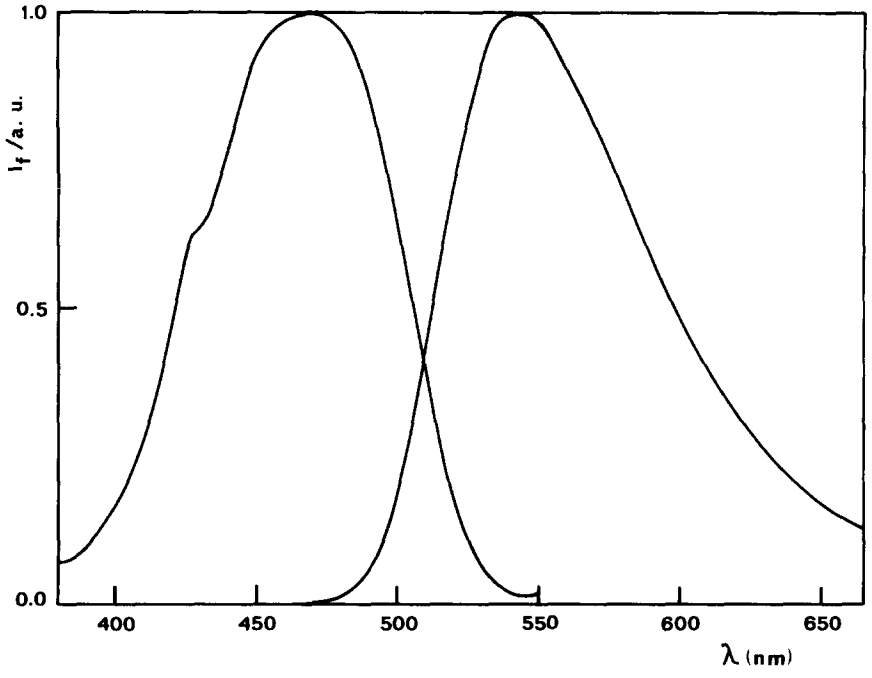

Fig. 2. Corrected excitation (λ_{em} = 467 nm) and emission (λ_{ex} = 543 nm) spectra of NBD-DG (10^{-5} M) incorporated in EYL membranes (5 × 10^{-4} M) at 25°C.

transition moment of the fluorophore. A concomitant decrease of both the mean lifetime (with the exception for chloroform, τ = 9.76 ns) and of the quantum yield were also observed. These results are similar to the ones reported for an NBD derivative of phosphatidylethanolamine, where the NBD label is bound to the lipid headgroup [17]. The lifetimes reported for this latter probe in ethanol (τ = 6.7 ns) and water (τ = 1.1 ns) are also very close to the ones shown in Table 1. It should be stressed that at variance with Arsinte et al. [17], we also observe complex decays for the probe even in homogeneous solvents. In this way, due to the complex photophysics of the NBD chromophore, the existence of different environments in the membrane cannot be inferred from the complex lifetime data observed.

Table 1

Maximum excitation (λ_{ex}) and emission (λ_{em}) wavelengths (corrected spectra), steady-state anisotropy (r) and mean lifetimes ($\bar{\tau}$) of NBD-DG (10^{-5} M) in homogeneous media and incorporated in different phospholipid vesicles (5 × 10^{-4}M).

Medium	λ_{ex} (nm)	λ_{em} (nm)	r	$\bar{\tau}$ (ns)
Hexane	430	507	0.005	6.17
Chloroform	486	519	—	9.76
Ethanol	469	530	—	5.81
Water	478	550	—	1.08
EYL	462	543	0.135	6.40
PS	462	543	0.127	—
DPPC 25°C	462	543	0.156	6.09
DPPC 50°C	462	543	0.084	—

The fluorescence parameters are insensitive to the type of lipid where the probe is incorporated, as shown in Table 1, namely the absorption and emission wavelengths. This is evidence that in all cases the probe location in the membrane is identical and, in addition, it is incorporated in a polar environment, near the lipid/water interface, since the emission wavelength (543 nm) is between those

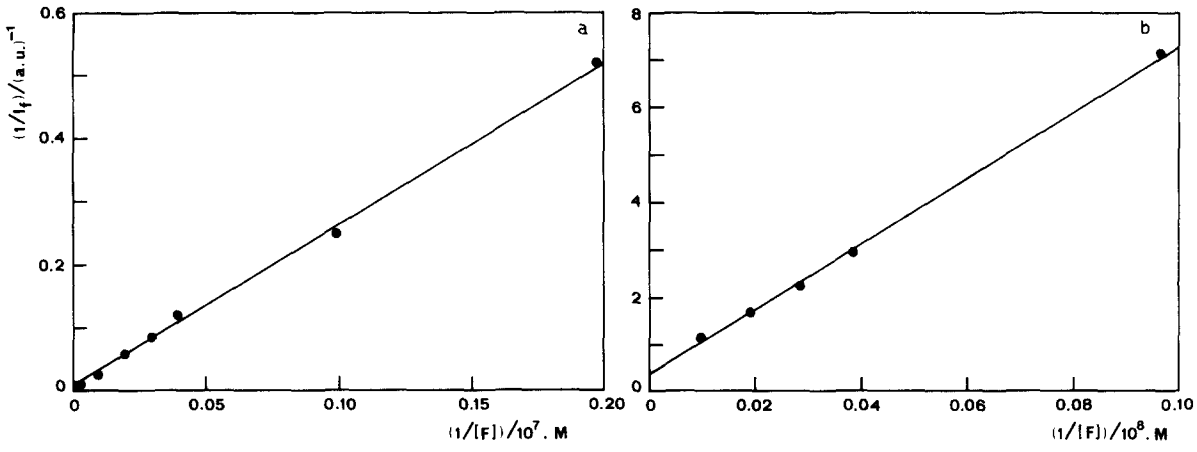

Fig. 3. Double-reciprocal representation of the fluorescence intensity (I_f) vs. probe concentration ([F]) for EYL membranes containing NBD-DG (panel a) and NBD-PC (panel b), at 25°C. Phospholipid concentration was 4×10^{-4} M.

obtained for ethanol (530 nm) and water (550 nm). It is common that for probes where the polar chromophore is located at the end of a lipidic aliphatic chain, it approaches the surface instead of being buried inside the membrane. A similar observation was reported [18,19] for NBD labels placed at the end of fatty acyl chains of phosphatidylcholines. Because of this fact a certain caution should be exercised before extending the conclusions on dynamics and aggregation of NBD-diacylglycerols to unlabelled diacylglycerols.

The anisotropy values obtained for the probe incorporated in model membranes (Table 1) are in the range 0.13–0.16. These moderately high values, due to a restricted depolarization dynamics, are compatible with a probe location near the membrane interface. For DPPC in the gel state, the highest anisotropy value is obtained ($r = 0.156$), this anisotropy being lower for the other two lipids in the liquid-crystalline state, PS and EYL. The anisotropy value for DPPC above the phase transition temperature is the lowest. As an increase in temperature could only decrease the fluorescence lifetime and in this way increase the anisotropy value, this result is evidence that in DPPC in the liquid-crystalline state (at 50°C) the probe motion is more facilitated regarding the other two lipids (at 25°C).

4.2. *Fluorescence self-quenching*

Both for NBD-DG and NBD-PC, an efficient fluorescence self-quenching was observed upon increasing its concentration in the membrane, a downward curvature of fluorescence intensity (I_f) vs. concentration being obtained. When the reciprocal intensity $1/I_f$ is plotted vs. the reciprocal concentration $1/[F]$ (see Eq. 12), linear relationships were obtained, as shown in Fig. 3a for the self-quenching of NBD-DG and in Fig. 3b for NBD-PC, when these probes were incorporated in EYL membranes.

In all these experiments, no spectral evidence of ground state association was obtained, for the highest probe concentration used.

A fluorescence self-quenching has been reported for *N*-NBD-phosphatidylethanolamine in a study where this interaction was used to monitor Ca^{2+}-induced fusion of vesicles [20], but rate constants were not presented in that work.

From the slopes and intercepts of these plots, together with the lifetime value $\tau = 6.4$ ns, the bimolecular quenching rate constants k_m were obtained and are presented in Table 2. The bimolecular rate constant, as described under Theory, is given by Eq. 5; the values of diffusion coefficients D obtained in this way are presented in

Table 2
Anistrophy at infinite dilution (r_d), limiting anistropy in the high concentration range (r_c), bimolecular rate constant of quenching (k_m, in M^{-1} s^{-1}) and lateral diffusion coefficient (D, in cm^2 s^{-1}) for NBD-DG and NBD-PC incorporated in EYL vesicles, at 25°C.

Probe	r_d	r_c	k_m	D
NBD-DG	0.13	0.10	1.6×10^9	2.1×10^{-6}
NBD-PC	0.12	0.07	4.2×10^9	6.6×10^{-6}

Table 2, the value of NBD-DG being slightly lower than that of NBD-PC. These coefficients are one or two orders of magnitude higher than those obtained from FRAP techniques, and this point will be addressed later in this work. It should be emphasized that a collisional mechanism where no ground-state interactions are considered (static quenching) correctly describes the experimental results. This is further supported from transient state data in highly doped membranes with the related probe *N*-NBD-phosphatidylethanolamine. Working out the lifetime values of Fig. 4. in Arsinte et al. [17], a value of $k_m = 2.2 \times 10^9$ $M^{-1}s^{-1}$ is obtained close to the ones shown in Table 2.

In this way we can conclude from our results that no significant aggregation of NBD-DG is present in the model membrane under study.

4.3. Energy transfer (migration)

Both for NBD-PC and NBD-DG, a decrease in anisotropy is observed upon increasing the probe-lipid ratio, as shown in Fig. 4a,b. In these plots the anisotropy values are normalized to the value obtained in dilute solutions (r_d) (probe:lipid = 1:1000).

The variation of anisotropy is due to the energy migration (dipolar mechanism); radiative transport contribution is negligible because of the low optical densities, and, in addition, 5 mm cuvettes were used.

For both probes, limiting values of anisotropy in the higher concentration range (r_c) are clearly defined. In Table 2 the absolute values obtained for infinite dilutions (r_d) and for the limit in the high concentration (r_c) are presented. This last value is higher for NBD-DG than for NBD-PC.

The energy migration efficiency should decrease the fluorophore anisotropy, without affecting its lifetime. In agreement we verified that in the dilute concentration range where the anisotropy study

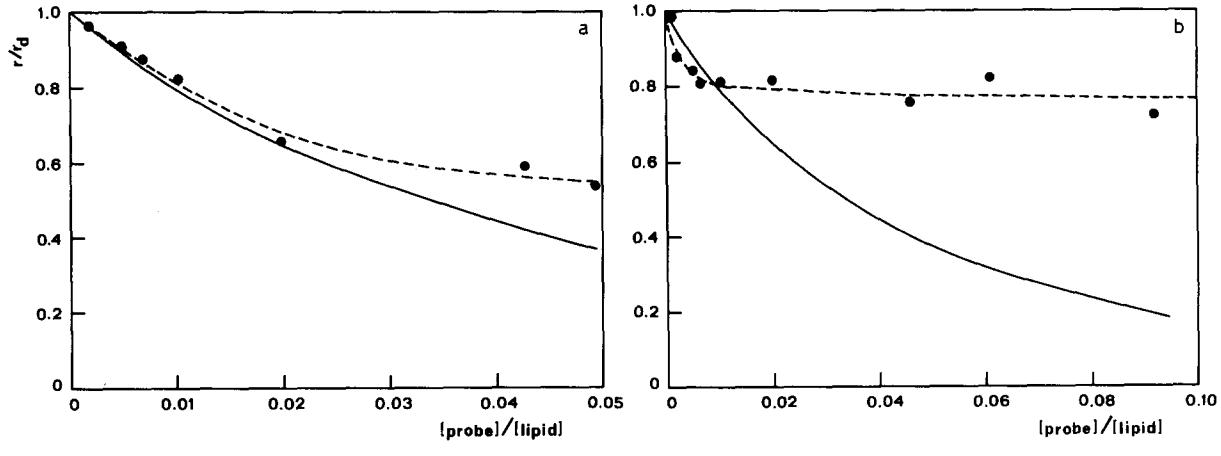

Fig. 4. Dependence of the ratio of the anisotropy to the anisotropy at infinite dilution (r/r_d) vs. the probe/lipid ratio for NBD-PC (panel a) and NBD-DG (panel b) incorporated in EYL membranes, at 25°C. Phospholipid concentration was kept constant to 4×10^{-4} M. Solid lines are based on Monte-Carlo simulation (Snyder and Freire, [23]).

was carried out (Fig. 4a,b), the probe lifetime is invariant. As shown in Fig. 2, there is a considerable spectral overlap of absorption and emission for the NBD-DG chromophore in membranes, and from Eq. 3 a Förster critical radius $R_0 = 28$ Å was determined, pointing to an efficient electronic energy migration in these probes. For the purpose of R_0 determination, the quantum yield for the parent probe NBD-PC in MLV $\phi = 0.48$ was considered, and the molar absortivity ϵ was taken from the literature [6].

Because of the explicit distance dependence (r^{-6}) of the dipolar mechanism, information on the distance distribution function of molecules can be obtained; however, the theoretical modelling of the fluorescence anisotropy variation is not trivial, and only approximate models are available. Simulations for energy migration in two dimensions were recently presented [21], as well as experimental work in model systems of membranes [22].

The most immediate approach to the quantitative variation of anisotropy is the work of Snyder and Freire [23]. These authors used a Monte-Carlo simulation technique to predict the decrease of anisotropy in a random distribution of probes in two dimensions, assuming also random (isotropic) orientation of the transition moments. For practical purposes the anisotropy variation upon probe concentration was fitted to a fourth-order polynomial, and its application to NBD-PC and NBD-DG in EYL model membranes is also shown in Fig. 4a,b. For NBD-PC (Fig. 4a), the theoretical expectations verify the experimental values, a deviation being noticed for the higher probe concentrations. This deviation is rationalized on the basis of the restricted depolarization dynamics of the probe incorporated in the membrane, at variance with the model assumption where random (isotropic) transition dipoles were assumed. It should be stressed that in our model systems there is no effect of bilayer curvature affecting the energy transfer efficiency, i.e. the anisotropies, as shown in the literature [24,25]. In addition, the meaning of the anisotropy value at the plateau region (r_c in Table 2) is very interesting: it should be related and close to the limiting anisotropy r_∞ [26] of the probe in the membrane; as shown in the work of Johansson et al. [21], a residual anisotropy is obtained for non-isotropically oriented dipoles. Upon increasing the fluorophore concentration a very efficient energy transfer is operative, but the maximum depolarization allowed by the system is controlled by the wobbling diffusion angle of the probe. This experiment would then be a way of obtaining information on r_∞ from energy migration experiments. It should be stressed that the observed plateau is not affected by an anisotropy increase due to collisional self-quenching (because of lifetime reduction). Even for the higher concentration range this effect is negligible. Interestingly, the value for NBD-DG ($r_c = 0.10$) (Table 2) is higher than the one for NBD-PC ($r_c = 0.07$).

The results for NBD-DG (Fig. 4b) show that in the dilute range the energy migration is more efficient than the theoretical prediction. This could suggest a non-random distribution of probes, i.e. some segregation of NBD-DG into domains would exist. Instead we think that it should be due to the higher value of r_∞ for this probe, i.e. the dipoles are already in a very favourable orientation for transfer, the orientational factor k^2 in Eq. 3 being greater.

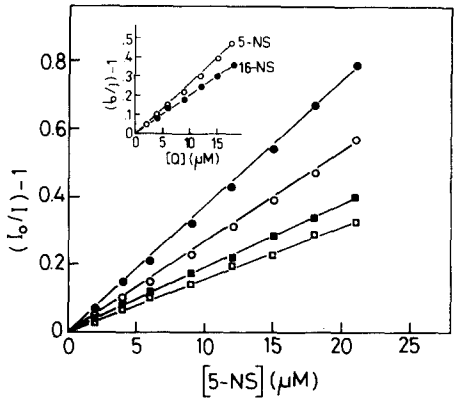

Fig. 5. Stern-Volmer plot of quenching of NBD-DG fluorescence by 5-NS at 25°C in EYL vesicles, at different membrane fractional volumes (α_m): 0.28×10^{-3} (□); 0.21×10^{-3} (■); 0.14×10^{-3} (○) and 0.10×10^{-3} (●). The NBD-DG to phospholipid ratio was kept at 1:100 (mol/mol). Insert shows a comparison of the quenching produced by 5-NS and 16-NS at a fractional volume, α_m, of 0.14×10^{-3}.

4.4. Intermolecular quenching

The quenching effect of the membrane probes 5-doxylstearate (5-NS) and 16-doxylstearate (16-NS) on NBD-DG fluorescence is shown in the inset of Fig. 5. The quenching kinetics is described by a collisional mechanism, as shown by the linearity of the Stern-Volmer plots. It can be seen that 5-NS, which has its nitroxide group at carbon-5, quenches NBD-DG fluorescence more effectively than 16-NS, which has its nitroxide group at carbon-16. These probes were used before in a number of similar studies designed to determine the location of chromophores in membranes [27,28]. The finding that 5-NS is a more efficient quencher than 16-NS is compatible with a location of the NBD fluorophore near the lipid-water interface, in agreement with the photophysical parameters of this probe (see above).

The calculation of the lateral diffusion coefficient of NBD-DG when incorporated into phospholipid vesicles can be approached through studies of the quenching of NBD-DG fluorescence by 5-NS, as described previously (Eqs. 4 and 5).

Fig. 5. shows Stern-Volmer plots for the quenching of NBD-DG fluorescence, when incorporated in EYL vesicles, by 5-NS, at different lipid concentrations. From these plots apparent bimolecular quenching constants (k_{app}) values were calculated. The fit of Eq. 4 to those values is shown in Fig. 6, a bimolecular quenching rate constant $k_m = 1.1 \times 10^9\ M^{-1}\ s^{-1}$ and a partition coefficient of quencher $P = 9.2 \times 10^3$ being recovered. In order to calculate the lateral diffusion coefficient of NBD-DG in the membrane we used in the Smoluchowski equation (Eq. 5), a value $D_q = 2.5 \times 10^{-6}\ cm^2\ s^{-1}$ [15]. In this way $D_p = 3.5 \times 10^{-6}\ cm^2\ s^{-1}$ is determined, close to the one obtained from the self-quenching study (Table 2). The partition coefficient P of 5-NS is also of the same order of magnitude as that previously reported [28].

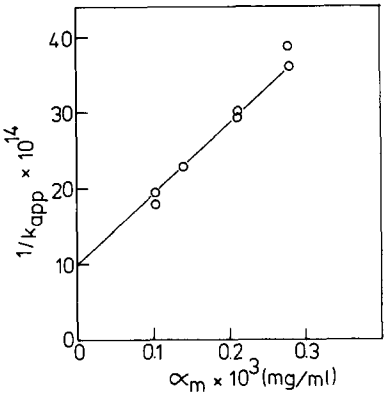

Fig. 6. Plot of $1/k_{app}$ vs. membrane fractional volumes (α_m), using values from Fig. 5. Points corresponding to two different sets of experiments are shown.

We are aware that these diffusion coefficients are two orders of magnitude higher than those obtained by fluorescence recovery after photobleaching (FRAP) techniques. This discrepancy is well known [29], and recently was addressed in detail by Vaz and Almeida [30]; these authors compared the high values obtained from short-range techniques (e.g. quasielastic neutron scattering) with those of long-range diffusion (FRAP), and rationalized them within the model of the free-volume for diffusion in a lipid bilayer. Fluorescence quenching is a specific bimolecular reaction that senses an intermediate range (several lipid diameters), and the derived diffusion coefficients from experiment are model-dependent.

Membranes are a quasi-two-dimensional medium, and models for fluorescence quenching based on this dimensionality were presented in the literature [31–33], as well as applications of the theory of random walks in fractal domains [34]. At variance with diffusion in three dimensions, when reducing the dimension of the system, no steady state is attained, i.e. a time-independent rate constant is not reached after an initial transient period, and non-linear Stern-Volmer plots are obtained [33]. It should be stressed that differences in D values, with respect to various models, are more significant for probes with long lifetimes, e.g. pyrene. On the other hand, when using a three-dimensional analysis in a two-dimension situation, underestimated values of D are obtained [35], i.e. the diffusion coefficients obtained in this work would still be higher. A contribution of static quenching would imply the determination of overestimated D values. However, in our study this situation is contradicted by the following facts: (i) the existence of identical lipid domains in

different situations (self-quenching:probe-probe; nitroxide-quenching:probe-quencher) should be invoked and (ii) as previously indicated from transient state data for self-quenching in highly doped membranes with a related probe (Fig. 4 of Arsinte et al. [17]), an identical bimolecular rate constant is obtained.

5. Conclusions

This work describes a fluorescence study of a diacylglycerol labelled with the NBD probe, incorporated in model membranes. In order to understand any specific effects due to the presence of the label and not associated to the DG structure, a concomitant study of an NBD-PC was carried out.

Photophysical parameters of both probes are very similar, and from its study in homogeneous media it can be concluded that the NBD-chromophore is located near the membrane surface. In addition, non-specific effects due to the type of phospholipid were noticed; fluorescence excitation and emission wavelenghts and lifetimes are independent of the type of lipid where the probe is incorporated.

Fluorescence self-quenching of the NBD-DG and NBD-PC probes were studied in EYL, the data being described by a modified Stern-Volmer kinetics which only considers a collisional mechanism. The diffusion coefficients obtained for both probes are in the range of $D = 2\text{–}6 \times 10^{-6}$ cm^2 s^{-1}, this study being evidence that no significant aggregates of fluorescent diacylglycerol exist in the membrane; this conclusion was also supported by working out transient state data for a similar probe in the literature [17]. Nevertheless, this cannot rule out the possibility that in biological membranes with heterogeneous lipid composition, and where different lipid domains may be present, DGs might be preferentially concentrated in some of these domains.

An efficient energy migration ($R_0 = 28$ Å) was observed for these probes. The experimental data of the anisotropy dependence on probe concentration in model membranes was compared with a model that considers random distribution in two dimensions and isotropic orientation of the transition moments. The theoretical expectations were verified in the dilute region, and, interestingly, instead of complete depolarization, values of 0.07 (NBD-DG) and 0.10 (NBD-PC) were obtained at high probe concentrations. This incomplete depolarization is due to the limited wobbling cone of diffusion of the probe in the membrane, i.e. the existence of an anisotropy at infinite time r_∞. It is very interesting that information on this parameter could be obtained directly from an energy migration study in a membrane.

The depolarization data on the dilute range again are evidence for a random distribution of NBD-DG, i.e. there is no significant aggregation of the probe.

The surface location of the fluorophore of NBD-DG probe was further confirmed from a study of its fluorescence quenching with the spin labels 5-NS and 16-NS, a diffusion coefficient $D = 3.5 \times 10^{-6}$ cm^2 s^{-1} being obtained in agreement with those of the self-quenching study.

It should be stressed that NBD-DG has a diffusion coefficient similar to that of a phospholipid such as NBD-PC, and hence it can difuse easily in the membrane. The rapid movement of DGs may have significance, since it is known that their concentration in biological membranes is very low, reaching at most transient levels of 2 mol% after stimulation [36]. Hence if it is produced in very limited amounts, at a site in the membrane separated from the point where it should act, its capacity to diffuse rapidly would be an advantage to shorten the delay time between its generation due to an external stimulus to the cell and the generation of a biological signal as a response.

6. Acknowledgement

This work was supported by INIC, Portugal (project 1G-CQFM), by Acción Integrada Hispano-Portuguesa (59 B, Area 4) and by a grant from DGICYT, Spain (grant no. PM-90/0044). A research grant from INICT, Portugal, to M.C. is acknowledged.

7. References

1 Y. Nishizuka (1984) Nature 308, 693–698.
2 A. Ortiz, J. Villalaín and J.C. Gómez-Fernández (1988) Biochemistry 27, 9030–9036.

3 M.J. Berridge (1987) Annu. Rev. Biochem. 56, 159–193.
4 D.E. Chalpin and A.M. Kleinfeld (1983) Biochim. Biophys. Acta 731, 465–474.
5 G.R. Bartlett (1959) J. Biol. Chem. 234, 466–468.
6 R.A. Cerione, R.E. McCarthy and G.G. Hammes (1983) Biochemistry 24, 4097–4108.
7 D.F. Eaton (1988) J. Photochem. Photobiol. 82, 523–530.
8 M. Zuker, A.G. Szabo, L. Bramall, D.T. Krajkarski and B. Selinger (1985) Rev. Sci. Instrum. 56, 14–22.
9 M.N. Berberan-Santos and M.J.E. Prieto (1987) J. Chem. Soc., Faraday Trans. II, 83, 1391–1409.
10 L. Davenport, R.E. Dale, R.H. Bisby and R.B. Cundall (1985) Biochemistry 24, 4097–4108.
11 J.R. Lakowicz and D. Hogen (1980) Chem. Phys. Lipids 26, 1–40.
12 J.Q. Umberger and V.K. Lamer (1945) J. Am. Chem. Soc. 67, 1099–1109.
13 J.T. Edward (1970) J. Chem. Educ. 47, 261–270.
14 S.A. Green, D.J. Simson, G. Zhou, P.S. Ho and N.V. Blough (1990) J. Am. Chem. Soc. 112, 7337–7346.
15 R. Fato, M. Battino, M. Degli Esposti, G. Parenti-Castelli and G. Lenaz (1986) Biochemistry 25, 3376–3390.
16 A. Chattopadhyay (1990) Chem. Phys. Lipids 53, 1–15, and references cited therein.
17 T. Arsinte, A. Cudd and K. Hildenbrand (1986) Biochim. Biophys. Acta 860, 215–228.
18 A. Chattopadhyay and E. London (1987) Biochemistry 26, 39–45.
19 A. Chattopadhyay and E. London (1988) Biochim. Biophys. Acta 938, 24–34.
20 D. Hoekstra (1982) Biochemistry 21, 1055–1061.
21 L.B.-A. Johansson, S. Engström and M. Lindberg (1992) J. Chem. Phys. 96, 3844–3856 (and references cited therein).
22 B. Kalman and L.B.-A. Johansson (1992) J. Chem. Phys. 96, 185–190.
23 B. Snyder and B. Freire (1982) Biophys. J. 40, 137–148.
24 B.K.-K. Fung and L. Stryer (1978) Biochemistry 17 (24) 5241–5248.
25 J. Eisinger, W.E. Blumberg and R.E. Dale (1981) Ann. N.Y. Acad. Sci. 366, 155–157.
26 K. Kinosita, S. Kawato and A. Ikegami (1977) Biophys. J. 20, 289–305.
27 E. Blatt, R.C. Chatelier and W.H. Sawyer (1984) Photochem. Photobiol. 39, 477–483.
28 F.J. Aranda, A. Coutinho, M.N. Berberan-Santos, M.J.E. Prieto and J.C. Gómez-Fernández (1989) Biochim. Biophys. Acta 985, 26–32.
29 K. Rajarathnam, J. Hochman, M. Schindler and S. Ferguson-Miller (1989) Biochemistry 28, 3168–3176.
30 W.L.C. Vaz and P.F. Almeida (1991) Biophys. J. 60, 1553–1554.
31 C.S. Owen (1975) J. Chem. Phys. 62, 3204–3207.
32 J.M. Vanderkooi, S. Fischkoff, M. Andrich, F. Podo and C.S. Owen, (1976) J. Chem. Phys. 63, 3661–3666.
33 F. Caruso, F. Grieser, A. Murphy, P. Thistlewaite, R. Urkuhart, M. Almgren and E. Wistus (1991) J. Am. Chem. Soc. 113, 4838–4843.
34 G. Duportail, J.-C. Brochon and P. Lianos (1992) J. Phys. Chem. 96, 1460–1463.
35 M. Almgren (1991) in: M. Grätzel, K. Kalyanasundaram (Eds.), Kinetics and Catalysis in Microheterogeneous Systems, Marcel Dekker, New York, pp. 63–113–113.
36 J. Preiss, C.R. Loomis, W.R. Bishop, R. Stein, J.E. Niedel and R.M. Bell (1986) J. Biol. Chem. 261, 8597–8600.